Matched-Filter Bound for Binary Signaling Over Dispersive Fading Channels With Receive Diversity

Hafez Hadinejad-Mahram, Dirk Dahlhaus, and Dirk Blömker

***Abstract*—The matched-filter bound (MFB) for continuously dispersive Rayleigh fading channels with receive diversity is derived. The treatment is quite general, as the case of discrete multipath channels with correlated fading is included in our model as a special case, and we impose no constraints with regard to the selectivity of the channel. It is assumed that a statistical characterization of the channel is available through its direction-delay-Doppler power spectral density. The Karhunen–Loève expansion for vector processes is used to describe the received signal. The MFB is analyzed with respect to several parameters characterizing the mobile radio channel, the waveform, and the antenna configuration.**

***Index Terms*—Antenna diversity, error probability.**

I. Introduction

In recent years, an increasing interest in theoretical evaluation of the bit-error probability (BEP) performance of systems operating in fading environments has occurred. However, the derivation of analytical expressions for the BEP performance of sophisticated receiver algorithms in fading environments is often quite cumbersome. An alternative is to resort to bounds for these expressions which are, in general, based on certain assumptions. One such bound is the so-called *matched-filter bound* (MFB) which describes the performance for uncoded and intersymbol interference (ISI)-free signaling in additive white Gaussian noise (AWGN). It is assumed that the receiver is ideally synchronized to the received signal and that it has perfect knowledge of the fading channel. The MFB is a theoretical lower bound which is, in general, not achievable by practical systems due to, e.g., ISI and inaccuracies of channel estimation. However, it is a useful tool for evaluating and designing digital communication systems.

Results of BEP performance analysis of receivers employing an antenna array (AA) have been reported in a number of papers [1]–[8]. Pierce and Stein [1] provide one of the earliest works on this subject. In [2] and [6], the MFB is derived for continuously dispersive Rayleigh fading channels where [2] considers slow, and [6], fast fading. However, the restriction to independent antenna branches prevents insight into several important aspects of system design. Aalo [3] investigates the BEP performance in Nakagami-m fading. However, the analysis is of limited applicability, since it is based on specific (uniform and Gaussian) correlation models. The generalization to arbitrary correlation models is provided by Lombardo *et al.* [4] and Zhang [5]. Note that in [1] and [3]–[5], a frequency-flat slowly fading channel is assumed, which limits the applicability of their results. Ling [7] and Visoz and Bejjani [8] derive the MFB for an arbitrary correlated, frequency-selective discrete-time slowly Rayleigh fading channel.

In this letter, we derive the MFB for the multiple-antenna case under very general conditions by a straightforward extension of the approach in [9], and investigate its behavior with respect to the parameters characterizing the mobile radio channel, the waveform used, and the properties of the receiving AA. Our approach extends the aforementioned works on the BEP performance of multiple-antenna systems in several ways. First, we allow for channel selectivity in all three dimensions, space, time, and frequency at the same time. Second, the widely-used discrete time-invariant tapped-delay-line model [10] can be obtained as a special case. Thus, we generalize [6] to arbitrary correlated antenna branches and [8] to continuously dispersive channels with nonnegligible Doppler dispersion. In view of this, we provide a unification of previously known results. Finally, by adopting Fleury's channel description [11] with the three-dimensional (3-D) direction parameter $\vec{\Omega}$, we are able to formulate general expressions for the MFB dropping the restrictive, yet widespread, assumption of horizontally propagating waves.

In Section II, we discuss the system model. Section III is devoted to the derivation of the MFB. We first consider the problem in its general formulation before briefly discussing two special cases. In Section IV, we analyze the MFB for several examples. Finally, our concluding remarks are presented in Section V.

II. System Model

We consider a radio communication system with one transmit and M receive antennas with identical element patterns. We use the channel description in [11] which extends Bello's wide-sense stationary uncorrelated scattering channel model [12] to include direction dispersion. It is characterized by the direction-delay-Doppler (DDD) spread function $h(\vec{\Omega},\tau,\nu)$ [11]. Here, $\vec{\Omega} = [\cos(\varphi)\sin(\theta),\sin(\varphi)\sin(\theta),\cos(\theta)]^{\mathrm{T}}$ is a unit vector[1] describing a direction in a coordinate system with an arbitrary origin, and φ and θ denote the azimuth and elevation angle, respectively. Furthermore, τ,ν, and $(\cdot)^{\mathrm{T}}$ denote delay, Doppler

[1]We denote space vectors in $\mathbb{R}^3$ by placing a small arrow above the corresponding variables, e.g., $\vec{x}$. Other vectors are indicated by boldface letters.

Paper approved by G. M. Vitetta, the Editor for Equalization and Fading Channels of the IEEE Communications Society. Manuscript received February 2, 2003; revised November 4, 2004.

H. Hadinejad-Mahram was with the Institute of Communications Engineering, Aachen University, 52056 Aachen, Germany. He is now with Telecomino Co., Tehran 19149-65351, Iran (e-mail: hafez@gmx.de).

D. Dahlhaus is with the Communication Technology Laboratory, Swiss Federal Institute of Technology (ETH) Zurich, CH-8092 Zurich, Switzerland (e-mail: dahlhaus@nari.ee.ethz.ch).

D. Blömker is with the Institut für Mathematik, Aachen University, 52056 Aachen, Germany (e-mail: bloemker@instmath.rwth-aachen.de).

Digital Object Identifier 10.1109/TCOMM.2004.838675

frequency, and transposition, respectively. The zero-mean complex Gaussian process $h(\vec{\Omega},\tau,\nu)$ is assumed to be an orthogonal stochastic measure [11], i.e.,

$$\mathrm{E}\{h(\vec{\Omega},\tau,\nu)h(^*\vec{\Omega}',\tau',\nu')\} = P(\vec{\Omega},\tau,\nu)\delta(\vec{\Omega}-\vec{\Omega}')\delta(\tau-\tau')\delta(\nu-\nu') \quad (1)$$

where $P(\vec{\Omega},\tau,\nu)$, $\mathrm{E}\{\cdot\}$, and $(\cdot)^*$ denote the power spectral density (PSD) of $h(\vec{\Omega},\tau,\nu)$, expectation, and complex conjugation, respectively. Without loss of generality, we assume $h(\vec{\Omega},\tau,\nu)$ to be normalized such that $\iiint P(\vec{\Omega},\tau,\nu)\,\mathrm{d}\vec{\Omega}\,\mathrm{d}\tau\,\mathrm{d}\nu = 1$, where integrals without explicit limits are to be evaluated over the entire range of the corresponding variables.

Upon transmission of $s(t)$ the complex baseband channel output at some point $\vec{x}$ is given by

$$r(\vec{x},t) = \int_{\mathbb{R}}\int_{\mathbb{R}}\int_{||\vec{\Omega}||=1} s(t-\tau)h(\vec{\Omega},\tau,\nu)\exp(\jmath 2\pi\lambda^{-1}\vec{\Omega}\cdot\vec{x}) \times \exp(\jmath 2\pi\nu t)\,\mathrm{d}\vec{\Omega}\,\mathrm{d}\tau\,\mathrm{d}\nu \quad (2)$$

where $\vec{\Omega}\cdot\vec{x}$, $\{\vec{\Omega} : ||\vec{\Omega}|| = 1\}$, and λ, respectively, denote the inner product of $\vec{\Omega}$ and $\vec{x}$, the unit sphere and the carrier wavelength.[2] The received signal of the mth antenna located at $\vec{x}_m$ is given by $z_m(t) = r_m(t) + n_m(t), m = 1,\ldots,M$, where $r_m(t) = r(\vec{x}_m,t)$ and $n_m(t)$ is a complex zero-mean white Gaussian noise process. The noise processes of the antennas are assumed to be independent identically distributed (i.i.d.), i.e., $\mathrm{E}\{n_m(t+\varrho)n_\ell^*(t)\} = N_0\delta(\varrho)\delta_{m-l}$ where N_0, $\delta(\varrho)$, and δ_m denote, respectively, the noise PSD, the Dirac, and the Kronecker delta function, respectively.

III. Derivation of MFB

Let $s_0(t)$ and $s_1(t)$ be the complex envelopes of two waveforms used for transmitting binary symbols. Moreover, let $\rho_m(t)$ denote the response of the channel to the difference signal $\varsigma(t) = s_1(t) - s_0(t)$ at $\vec{x}_m$, i.e.,

$$\rho_m(t) = \iiint \varsigma(t-\tau)h(\vec{\Omega},\tau,\nu)\exp(\jmath 2\pi\lambda^{-1}\vec{\Omega}\cdot\vec{x}_m) \times \exp(\jmath 2\pi\nu t)\,\mathrm{d}\vec{\Omega}\,\mathrm{d}\tau\,\mathrm{d}\nu.$$

The optimum receiver for the mth antenna consists of a filter matched to $\rho_m(t)$ and a sampler. The samples from all antennas are then combined according to the maximal-ratio combining rule to form the decision variable. It can be shown [14] that the BEP conditioned on $h(\vec{\Omega},\tau,\nu)$ depends on the energy of the difference signal $\boldsymbol{\rho}(t) = [\rho_1(t),\ldots,\rho_M(t)]^{\mathrm{T}}$. The conditional BEP is given by [14] $P_{\mathrm{b}} = Q(\sqrt{2\gamma})$, where $Q(x) = \int_x^\infty (1/\sqrt{2\pi})\exp(-\zeta^2/2)\,\mathrm{d}\zeta$ and $\gamma = E_{\boldsymbol{\rho}}/(4N_0)$ is the *effective* signal-to-noise ratio (SNR) with the difference signal energy

$$E_{\boldsymbol{\rho}} = \int_{\mathcal{T}} \boldsymbol{\rho}^{\mathrm{H}}(t)\boldsymbol{\rho}(t)\,\mathrm{d}t = \sum_{m=1}^{M}\int_{\mathcal{T}} |\rho_m(t)|^2\,\mathrm{d}t$$

and $(\cdot)^{\mathrm{H}}$ denoting conjugate transposition. Note that $E_{\boldsymbol{\rho}}$ can be related to the (received) bit energy E_{b} of a specific modulation, e.g., $E_{\boldsymbol{\rho}} = 4E_{\mathrm{b}}$ for phase-shift keying (PSK) and $E_{\boldsymbol{\rho}} = 2E_{\mathrm{b}}$ for frequency-shift keying. The mean BEP results in

$$\bar{P}_{\mathrm{b}} = \mathrm{E}\{Q(\sqrt{2\gamma})\} = \int_0^\infty Q\left(\sqrt{\frac{x}{2N_0}}\right) p_{E_{\boldsymbol{\rho}}}(x)\,\mathrm{d}x \quad (3)$$

where $p_{E_{\boldsymbol{\rho}}}(x)$ is the probability density function of $E_{\boldsymbol{\rho}}$. Below, we first evaluate (3) for the general case of correlated antenna signals. Then we apply our results to the special cases of uncorrelated antenna signals and a separable DDD PSD.

A. Correlated Antenna Signals

We assume $\boldsymbol{\rho}(t) = 0$ for $t \notin \mathcal{T}$ where $\mathcal{T} \subset \mathbb{R}$ is finite. Then, we can expand $\boldsymbol{\rho}(t)$ for $t \in \mathcal{T}$ in the mean-square sense using a Karhunen–Loève expansion for vector signals [15], [16] according to

$$\boldsymbol{\rho}(t) = \sum_{i=1}^{\infty} \xi_i \boldsymbol{\psi}_i(t)$$

where $\xi_i = \int_{\mathcal{T}} \boldsymbol{\psi}_i^{\mathrm{H}}(t)\boldsymbol{\rho}(t)\,\mathrm{d}t$ and $\{\boldsymbol{\psi}_i(t)\}_{i=1}^{\infty}$ forms an orthonormal set of M-dimensional vector functions. Moreover, $\mathrm{E}\{\xi_i\xi_j^*\} = \int_{\mathcal{T}}\int_{\mathcal{T}} \boldsymbol{\psi}_i^{\mathrm{H}}(t)\mathbf{C}_{\boldsymbol{\rho}\rho}(t,u)\boldsymbol{\psi}_j(t)\,\mathrm{d}t\,\mathrm{d}u = \Lambda_i\delta_{i-j}$ where $\mathbf{C}_{\boldsymbol{\rho}\rho}(t,u) = \mathrm{E}\{\boldsymbol{\rho}(t)\boldsymbol{\rho}^{\mathrm{H}}(u)\}$ with $(t,u) \in \mathcal{T}\times\mathcal{T}$ is the kernel of the integral equation

$$\int_{\mathcal{T}} \mathbf{C}_{\boldsymbol{\rho}\rho}(t,u)\boldsymbol{\psi}_i(u)\,\mathrm{d}u = \Lambda_i\boldsymbol{\psi}_i(t) \quad (4)$$

and $\Lambda_i = \mathrm{E}\{|\xi_i|^2\}$ are the eigenvalues of $\mathbf{C}_{\boldsymbol{\rho}\rho}(t,u)$. Using (1), it can be shown that the components of $\mathbf{C}_{\boldsymbol{\rho}\rho}(t,u)$, defined by $C_{\rho_m\rho_\ell}(t,u) = \mathrm{E}\{\rho_m(t)\rho_\ell^*(u)\}$, are given by

$$C_{\rho_m\rho_\ell}(t,u) = \iiint \varsigma(t-\tau)\varsigma^*(u-\tau)P(\vec{\Omega},\tau,\nu) \times \exp(\jmath 2\pi\nu(t-u))\exp(\jmath 2\pi\lambda^{-1}\vec{\Omega}\cdot\Delta\vec{x}_{m\ell})\,\mathrm{d}\vec{\Omega}\,\mathrm{d}\tau\,\mathrm{d}\nu \quad (5)$$

where $\Delta\vec{x}_{m\ell} = \vec{x}_m - \vec{x}_\ell$. For $m = \ell$, (5) simplifies to

$$\begin{aligned} C_{\rho_\ell\rho_\ell}(t,u) &= \int\int \varsigma(t-\tau)\varsigma^*(u-\tau)P_1(\tau,\nu) \\ &\qquad \exp(\jmath 2\pi\nu(t-u))\mathrm{d}\tau\mathrm{d}\nu \\ &= C(t,u) \end{aligned}$$

where $P_1(\tau,\nu) = \int P(\vec{\Omega},\tau,\nu)\,\mathrm{d}\vec{\Omega}$ denotes the normalized scattering function of the channel [10].

Using Parseval's theorem, we have $E_{\boldsymbol{\rho}} = \sum_{i=1}^{\infty}|\xi_i|^2$ with $\xi_i, i = 1,2,\ldots$, being mutually independent zero-mean complex Gaussian variates with variances Λ_i. The characteristic function of $E_{\boldsymbol{\rho}}$ is [10]

$$\phi_{E_{\boldsymbol{\rho}}}(s) = \prod_{i=1}^{\infty}\phi_{|\xi_i|^2}(s) = \prod_{i=1}^{\infty}\frac{1}{1-s\Lambda_i}.$$

It can be represented by the partial fraction expansion (PFE)

$$\phi_{E_{\boldsymbol{\rho}}}(s) = \sum_{i=1}^{\infty}\sum_{n=1}^{q_i}\frac{\alpha_i^{(n)}}{(1-s\lambda_i)^n} \quad (6)$$

where $\{\lambda_i\}_{i=1}^{\infty}$ is the set of the distinct eigenvalues, q_i is the multiplicity of λ_i and $\alpha_i^{(n)}$ denote the PFE coefficients. The inverse Laplace transform of (6) yields

$$p_{E_{\boldsymbol{\rho}}}(x) = \sum_{i=1}^{\infty}\sum_{n=1}^{q_i}\frac{\alpha_i^{(n)}}{(n-1)!\lambda_i^n}x^{n-1}\exp\left(-\frac{x}{\lambda_i}\right). \quad (7)$$

[2]For the assumed case of identical antenna elements, the field pattern can be included in $h(\vec{\Omega},\tau,\nu)$ [11]. The extension to different antennas with individual patterns in (2) is straightforward [13].

Using (7) in (3) (cf. [10]) provides the MFB

$$\bar{P}_{\mathrm{b}} = \sum_{i=1}^{\infty} \sum_{n=1}^{q_i} \alpha_i^{(n)} p_i^n \sum_{v=0}^{n-1} \binom{n-1+v}{v} (1-p_i)^v \quad (8)$$

where $p_i = (1/2)(1 - \sqrt{\bar{\gamma}_i/(\bar{\gamma}_i+1)})$ and $\bar{\gamma}_i = \lambda_i/(4N_0)$ is the mean SNR in the ith signal dimension. For the mean SNR $\bar{\gamma}$, we have $\bar{\gamma} = \mathrm{E}\{\gamma\} = \sum_{i=1}^{\infty} \bar{\gamma}_i$. Note that in (8), $\bar{P}_{\mathrm{b}}$ depends only on the eigenvalues of $\mathbf{C}_{\boldsymbol{\rho}\boldsymbol{\rho}}(t,u)$ and N_0. As the infinite sum in (8) rules out its applicability, we derive arbitrarily tight upper and lower bounds, as in [9], which can be evaluated with finite computational effort.

The upper bound $\hat{P}_{\mathrm{b}}^{(N)}$ results from sorting $|\xi_i|^2$ in decreasing order of their variances and neglecting all signal dimensions with $\Lambda_i < \Lambda_N$ for some properly chosen N. Thus, we consider $\tilde{E}_{\boldsymbol{\rho}} = \sum_{i=1}^{N} |\xi_i|^2$ instead of $E_{\boldsymbol{\rho}}$ and obtain

$$\phi_{\tilde{E}_{\boldsymbol{\rho}}}(s) = \prod_{i=1}^{N} \frac{1}{(1-s\Lambda_i)} = \sum_{i=1}^{L} \sum_{n=1}^{q_i} \frac{\tilde{\alpha}_i^{(n)}}{(1-s\lambda_i)^n}$$

where L is the number of distinct eigenvalues, i.e., $N = \sum_{i=1}^{L} q_i$ and the PFE coefficient $\tilde{\alpha}_i^{(n)}$ is, in general, different from $\alpha_i^{(n)}$. In analogy to the derivation of (8), we obtain

$$\hat{P}_{\mathrm{b}}^{(N)} = \sum_{i=1}^{L} \sum_{n=1}^{q_i} \tilde{\alpha}_i^{(n)} p_i^n \sum_{v=0}^{n-1} \binom{n-1+v}{v} (1-p_i)^v. \quad (9)$$

If all λ_i are distinct ($q_i = 1$), (9) simplifies to

$$\hat{P}_{\mathrm{b}}^{(N)} = \sum_{i=1}^{N} \alpha_i p_i \quad \text{with} \quad \alpha_i = \tilde{\alpha}_i^{(1)} = \prod_{\substack{j=1 \\ j \neq i}}^{N} \lambda_i/(\lambda_i - \lambda_j).$$

The lower bound is given by (see [9] for details)

$$\check{P}_{\mathrm{b}}^{(N)} = \sum_{i=1}^{L} \sum_{n=1}^{q_i} \frac{\tilde{\alpha}_i^{(n)}}{(n-1)!\lambda_i^n} \int_{\mu_N}^{\infty} Q\left(\sqrt{\frac{x}{2N_0}}\right) \times (x-\mu_N)^{n-1} \exp\left(-\frac{x-\mu_N}{\lambda_i}\right) \mathrm{d}x$$

where $\mu_N = \sum_{i=N+1}^{\infty} \lambda_i$. Integration by parts provides

$$\check{P}_{\mathrm{b}}^{(N)} = \sum_{i=1}^{L} \sum_{n=1}^{q_i} \tilde{\alpha}_i^{(n)} \left[Q(\sqrt{2\check{\gamma}_N}) - \frac{\exp(-\check{\gamma}_N)}{2} \sqrt{\frac{\check{\gamma}_N}{\pi}} \times \sum_{v=0}^{n-1} \left(\frac{\mu_N}{\lambda_i}\right)^v U\left(v+1, v+\frac{3}{2}, \check{\gamma}_N(1+\bar{\gamma}_i^{-1})\right) \right]$$

where $\check{\gamma}_N = \mu_N/(4N_0)$ and $U(a,b,z)$ is the confluent hypergeometric function [17]. It can be easily shown [9] that both bounds converge to $\bar{P}_{\mathrm{b}}$ as N approaches infinity. Since the eigenvalues usually decrease rapidly toward zero, tight bounds can be calculated with a moderate number of eigenvalues. For the examples of Section IV, all eigenvalues $\lambda_i \geq 10^{-9}$ are taken into account, and the recursive scheme in [5] is used to calculate $\tilde{\alpha}_i^{(n)}$ for $q_i > 1$. In general, for the calculation of the relevant eigenvalues λ_i in (4), we can resort to numerical methods in standard software packages.

B. Uncorrelated Antenna Signals

If the distances between the array elements are sufficiently large, the received signals at any two different sensors can be assumed mutually uncorrelated, i.e., $\mathrm{E}\{\rho_m(t)\rho_\ell^*(u)\} = \mathrm{E}\{\rho_m(t)\}\mathrm{E}\{\rho_\ell^*(u)\} = 0$ for $m \neq \ell$. Thus, $\mathbf{C}_{\boldsymbol{\rho}\boldsymbol{\rho}}(t,u)$ simplifies to $\mathbf{C}_{\boldsymbol{\rho}\boldsymbol{\rho}}(t,u) = C(t,u)\mathbf{I}$, where $\mathbf{I}$ is the $M \times M$ identity matrix. Substituting this expression in (4) results in M decoupled scalar integral equations with the common kernel $C(t,u)$. Thus, the expression for the BEP in the case of uncorrelated antenna signals is obtained by replacing q_i with $w_i M$ where w_i is the multiplicity of the distinct eigenvalues of $C(t,u)$ and finding the corresponding PFE coefficients.

C. Separable Channels

The delay and Doppler-dispersion characteristics of the mobile radio channel depend, respectively, on the distribution of remote scatterers and the distribution of local-to-transmitter scatterers in conjunction with the relative motion between the transmitter and the receiver [18]. In contrast, direction dispersion is primarily caused by local-to-receiver scatterers, and to some extent by remote scatterers [18]. Therefore, for many practical scenarios, one can model the channel direction dispersion to be statistically independent of the delay and Doppler dispersion. For a justification based on experimental results, see [19]. Here, we assume that the DDD PSD can be factorized according to $P(\vec{\Omega},\tau,\nu) = P_2(\vec{\Omega})P_1(\tau,\nu)$. Substituting this in (5), we obtain $C_{\rho_m\rho_\ell}(t,u) = C(t,u)R(\Delta\vec{x}_{m\ell})$, where

$$R(\Delta\vec{x}) = \int P_2(\vec{\Omega}) \exp(j2\pi\lambda^{-1}\vec{\Omega}\cdot\Delta\vec{x})\, \mathrm{d}\vec{\Omega} \quad (10)$$

is referred to as the space correlation function. Thus, we have $\mathbf{C}_{\boldsymbol{\rho}\rho}(t,u) = C(t,u)\mathbf{R}$, where the $M \times M$ matrix $\mathbf{R}$ is defined by $[\mathbf{R}]_{m\ell} = R(\Delta\vec{x}_{m\ell})$, $m,\ell = 1,\ldots,M$, and the eigenvalues of $\mathbf{C}_{\boldsymbol{\rho}\rho}(t,u)$ are given as the product of the eigenvalues of $\mathbf{R}$ and the eigenvalues of $C(t,u)$.

IV. Analysis

To characterize the impact of the specific form of $P(\vec{\Omega},\tau,\nu)$ and different number of antennas M on the eigenvalues and the resulting mean BEP, we fix the mean received energy $\bar{E}_{\boldsymbol{\rho}} = \mathrm{E}\{E_{\boldsymbol{\rho}}\} = ME_{\varsigma}$, where E_{ς} denotes the energy of $\varsigma(t)$ and the last equation is due to the normalized PSD.

We assume a uniform linear array (ULA) with omnidirectional antennas. Furthermore, we use a 2-D propagation model, even though the expression derived for the BEP incorporates the 3-D case. This choice has been made since 3-D models are very rare in the open literature and may need further verification before being generally accepted. In contrast, 2-D models have been extensively used by many authors. Previous analyses have been based on uniform and/or Gaussian models for the azimuth PSDs which are observed, respectively, at the mobile station in densely built-up areas without a line of sight toward the base station [20], and at low-height base stations in urban environments [21]. However, the experimental investigation in [21] reveals that the latter occurs only in special cases, and suggests that a truncated Laplacian PSD is a more accurate model for typical macrocellular (urban as well as rural) environments. Thus, we use a truncated Laplacian PSD in the following analysis.

For 2-D propagation, the direction PSD $P_2(\vec{\Omega})$ simplifies to the azimuth PSD $P_2(\varphi)$, where φ is the azimuthal angle relative

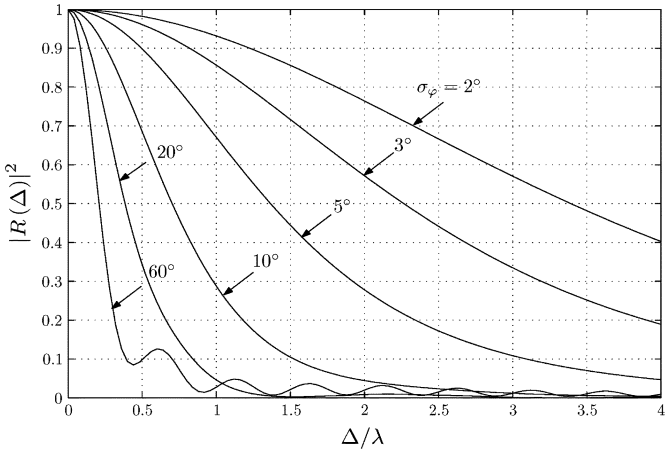

Fig. 1. PC versus Δ/λ for $\bar{\varphi} = 30°$ and different values of σ_φ.

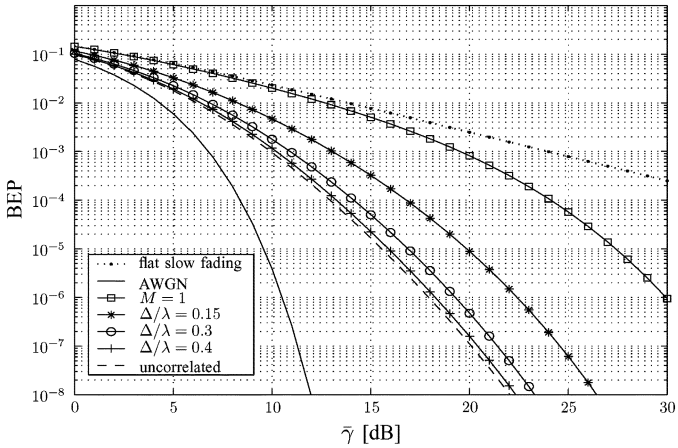

Fig. 2. BEP versus $\bar{\gamma}$ for different antenna spacings, a rectangular pulse, $M = 4, \sigma_\varphi = 60°, \bar{\varphi} = 30°, \sigma_\varphi/T = 10^{-2}, \nu_{\mathrm{D}}T = 10^{-3}$.

to an axis perpendicular to the line of the array. For the Laplacian case, we have

$$P_2(\varphi) = \kappa \exp(-|\varphi - \bar{\varphi}|/\sigma_\varphi), \quad \varphi \in [\bar{\varphi} - \pi, \bar{\varphi} + \pi)$$

where $\kappa = 1/(2\sigma_\varphi(1-\exp(-\pi/\sigma_\varphi)))$ is a normalization factor and $\bar{\varphi}$ and σ_φ are the mean angle-of-arrival (AOA) and the azimuth spread, respectively. For ULAs, $\Delta\vec{x}$ in (10) has a prescribed direction, i.e., $\Delta\vec{x}$ is confined along a straight line in the plane. In this case, we can rewrite (10) as

$$R(\Delta) = \int P_2(\varphi) \exp(\jmath 2\pi\lambda^{-1}\Delta\sin(\varphi))\,\mathrm{d}\varphi$$

where Δ denotes the antenna spacing. Evaluating the integral in terms of its real and imaginary parts we obtain, respectively

$$R_{\mathrm{R}}(\Delta) = J_0\left(2\pi\frac{\Delta}{\lambda}\right) + \sum_{m=1}^{\infty} J_{2m}\left(2\pi\frac{\Delta}{\lambda}\right)\frac{2\cos(m\bar{\varphi})}{1+(2m\sigma_\varphi)^2}$$

$$R_{\mathrm{I}}(\Delta) = \sum_{m=1}^{\infty} J_{2m-1}\left(2\pi\frac{\Delta}{\lambda}\right)\frac{2(c+1)\sin((2m-1)\bar{\varphi})}{(c-1)\left(1+(2m-1)^2\sigma_\varphi^2\right)}$$

with $c = \exp(\pi/\sigma_\varphi)$ and $J_m(x)$ denoting the mth-order Bessel function of the first kind. Fig. 1 shows the shape of $|R(\Delta)|^2$, commonly referred to as the power correlation (PC) [1], as a function of the normalized antenna spacing Δ/λ for $\bar{\varphi} = 30°$ and different values of σ_φ. For an angular spread of only 10°, a PC of 0.7, which is enough to yield a significant portion of the available diversity gain [22], is achieved at an antenna spacing of $\Delta = \lambda/2$. At a carrier frequency of 2 GHz, this corresponds to $\Delta = 7.5$ cm. Moreover, it is apparent that increasing the separation between the antenna elements reduces their correlation, and that the spacing required for a given PC decreases quickly as the angular spread increases.

In the following, pulses $\varsigma(t)$ with a temporal support T are considered. We illustrate the effects of the various parameters on the BEP of binary PSK as a function of $\bar{\gamma} = \bar{E}_{\boldsymbol{\rho}}/(4N_0) = \bar{E}_{\mathrm{b}}/N_0 = \bar{\gamma}_{\mathrm{b}}$ where $\bar{E}_{\mathrm{b}}$ and $\bar{\gamma}_{\mathrm{b}}$ are the mean bit energy and the mean SNR per bit, respectively. We assume a channel azimuth-delay-Doppler PSD of the form

$$P(\varphi,\tau,\nu) = \kappa\exp(-|\varphi-\bar{\varphi}|/\sigma_\varphi)\frac{\exp\left(-\frac{\tau}{\sigma_\tau}\right)}{\pi\sigma_\tau\sqrt{\nu_{\mathrm{D}}^2-\nu^2}} \qquad (11)$$

for $\tau \geq 0, |\nu| \leq \nu_{\mathrm{D}}, |\varphi - \bar{\varphi}| \leq \pi$, where σ_τ and ν_{D} denote the delay spread and the maximum Doppler frequency of the channel, respectively. In addition to the separability in Section III-C, $P_1(\tau,\nu)$ is assumed separable w.r.t. τ and ν in (11), due to usually independent mechanisms governing delay and Doppler-dispersion characteristics [23].

A. Effect of Antenna Spacing

A major issue in the design of AAs is the spacing of the sensors. The diversity gain should be maximized and at the same time, the array dimensions are to be kept as small as possible. Fig. 2 shows the BEP for different antenna spacings of a ULA with $M = 4$ elements, $\sigma_\varphi = 60°, \bar{\varphi} = 30°$, a rectangular pulse, $\sigma_\varphi/T = 10^{-2}$, and $\nu_{\mathrm{D}}T = 10^{-3}$. It can be seen that for a normalized antenna spacing of only $\Delta/\lambda = 0.3$, the biggest portion of the diversity gain is achieved. Moreover, at $\Delta/\lambda = 0.4$, the loss compared with the uncorrelated case is only a few tenths of a decibel. According to Fig. 1, with the above setting, the PC at $\Delta/\lambda = 0.3$ takes on 0.2. This implies that the previously quoted number 0.7 is a rather rough value for the considered channel. In a practical realization, we would probably choose a normalized antenna spacing of 0.3 instead of 0.15 (corresponding to a PC of 0.7), as this would yield a significant gain.

B. Impact of Angular Spread

Fig. 3 demonstrates the effect of the angular spread on the BEP for $M = 4, \Delta/\lambda = 0.5, \bar{\varphi} = 30°, \sigma_\varphi/T = 10^{-2}, \nu_{\mathrm{D}}T = 10^{-3}$, and a rectangular pulse. From Fig. 1, we expect the gain from $\sigma_\varphi = 3°$ over $\sigma_\varphi = 2°$ to be rather small, while a noticeable improvement can be predicted when going from $\sigma_\varphi = 5°$ to 10°, and from $\sigma_\varphi = 10°$ to 20°. Furthermore, we expect the improvement to be small for $\sigma_\varphi > 20°$. In Fig. 3, we find the quantitative confirmation of what we have been able to predict qualitatively.

C. Influence of Waveform on Time and Frequency Selectivity

Fig. 4 shows the BEP for four different pulse shapes including a rectangular pulse, a pseudonoise (PN) sequence $(+++--+--++)$ of rectangular pulses of the same total duration, and two extreme cases of a root raised-cosine (RRC) pulse [10]

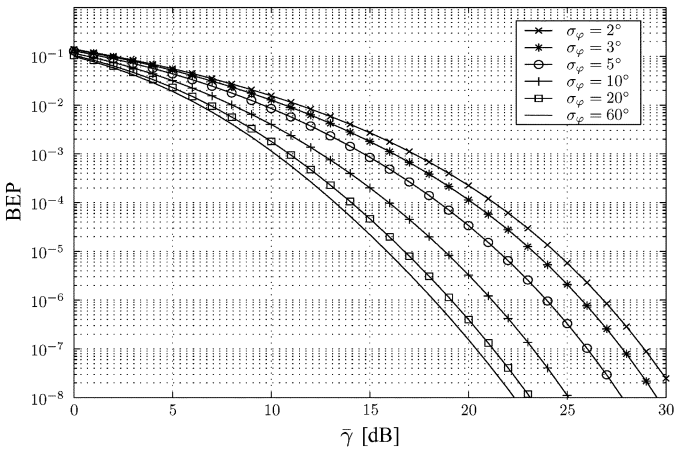

Fig. 3. BEP versus $\bar{\gamma}$ with different values of σ_φ for a rectangular pulse, $M = 4, \Delta/\lambda = 0.5, \bar{\varphi} = 30°, \sigma_\tau/T = 10^{-2}, \nu_{\mathrm{D}}T = 10^{-3}$.

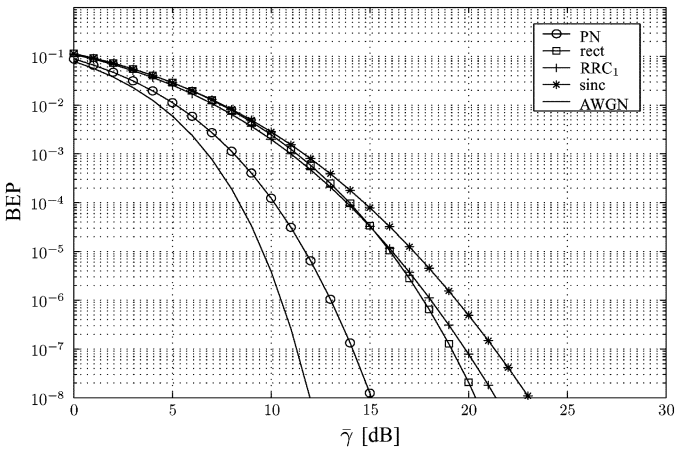

Fig. 4. BEP versus $\bar{\gamma}$ with different pulse shapes for $M = 2, \Delta/\lambda = 0.2, \bar{\varphi} = 30°, \sigma_\varphi = 30°, \sigma_\tau/T = 0.2$, and $\nu_{\mathrm{D}}T = 10^{-3}$.

with rolloff factors $\beta = 0$ (sinc) corresponding to a sinc-pulse and $\beta = 1$ (RRC_1). The number of antennas is $M = 2$, and the normalized antenna spacing is $\Delta/\lambda = 0.2$. The other parameters of the channel are $\bar{\varphi} = 30°, \sigma_\varphi = 30°, \sigma_\tau/T = 0.2$, and $\nu_{\mathrm{D}}T = 10^{-3}$. It is clear that this channel has a great potential of frequency selectivity (and thus diversity) because of the large extent of its delay PSD. It is seen that the PN waveform with its large bandwidth gives the lowest BEP, while the curves for the rectangular pulse and the two RRC pulses are rather close to each other. It is noteworthy that the curve for the PN waveform is only about 2 dB away from the AWGN curve at a BEP of 10^{-5}, even though there are only two receive antennas with a relatively high PC. This implies that the improvement is primarily due to frequency diversity.

V. Conclusion

The MFB for binary transmission with multiple receive antennas has been derived under general conditions for continuous Gaussian wide-sense stationary uncorrelated scattering channels. The bound is formulated in terms of the eigenvalues of the covariance function of the noiseless received signal vector process which, in turn, depends on the DDD PSD of the radio channel as well as the transmitted signal pulse. The analysis of the BEP for different antenna spacings, pulse shapes, and channel characteristics quantifies the diversity gain to be expected in different scenarios.

References

[1] J. Pierce and S. Stein, "Multiple diversity with nonindependent fading," in *Proc. IRE*, vol. 48, Jan. 1960, pp. 89–104.
[2] M. Clark, L. Greenstein, W. Kennedy, and M. Shafi, "Matched filter bounds for diversity combining receivers in digital mobile radio," *IEEE Trans. Veh. Technol.*, vol. 41, pp. 356–362, Nov. 1992.
[3] V. Aalo, "Performance of maximal-ratio diversity systems in a correlated Nakagami-fading environment," *IEEE Trans. Commun.*, vol. 43, pp. 2360–2369, Aug. 1995.
[4] P. Lombardo, G. Fedele, and M. Rao, "MRC performance for binary signals in Nakagami fading with general branch correlation," *IEEE Trans. Commun.*, vol. 47, pp. 44–52, Jan. 1999.
[5] Q. Zhang, "Maximal-ratio combining over Nakagami fading channels with an arbitrary branch covariance matrix," *IEEE Trans. Veh. Technol.*, vol. 48, pp. 1141–1150, July 1999.
[6] N. Baas and D. Taylor, "Matched filter bounds for wireless communications over Rayleigh fading dispersive channels," *IEEE Trans. Commun.*, vol. 49, pp. 1525–1528, Sept. 2001.
[7] F. Ling, "Matched filter bound for time-discrete multipath Rayleigh fading channels," *IEEE Trans. Commun.*, vol. 43, pp. 710–713, June 1995.
[8] R. Visoz and E. Bejjani, "Matched filter bound for diversity over frequency-selective Rayleigh-fading mobile channels," *IEEE Trans. Veh. Technol.*, vol. 49, pp. 1832–1845, Sept. 2000.
[9] T. Hunziker and D. Dahlhaus, "Bounds on matched filter performance in doubly dispersive Gaussian WSSUS channels," *Electron. Lett.*, vol. 37, no. 6, pp. 383–384, Mar. 2001.
[10] J. Proakis, *Digital Communications*, 3rd ed. New York: McGraw-Hill, 1995.
[11] B. H. Fleury, "First- and second-order characterization of direction dispersion and space selectivity in the radio channel," *IEEE Trans. Inform. Theory*, vol. 46, pp. 2027–2044, Sept. 2000.
[12] P. Bello, "Characterization of randomly time-variant linear channels," *IEEE Trans. Commun.*, vol. COM-11, pp. 260–393, Feb. 1963.
[13] B. H. Fleury and A. Kocian, "Bidirectional characterization of MIMO systems," in *Proc. 2nd Int. Workshop Research Directions in Mobile Communications and Services*, Grimstadt, Norway, Sept. 2002, pp. 51–54.
[14] M. Schwartz, W. Bennett, and S. Stein, *Communication Systems and Techniques*. New York: McGraw-Hill, 1966.
[15] A. Balakrishnan, "Estimation and detection theory for multiple stochastic processes," *J. Math. Anal. Appl.*, vol. 1, pp. 386–410, 1960.
[16] E. Kelly and W. Root, "A representation of vector-valued random processes," *J. Math. Phys.*, vol. 39, pp. 211–216, 1960.
[17] M. Abramowitz and I. Stegun, Eds., *Handbook of Mathematical Functions*. New York: Dover, 1981.
[18] A. Paulraj and C. Papadias, "Space–time processing for wireless communications," *IEEE Signal Processing Mag.*, pp. 49–83, Nov. 1997.
[19] K. Pedersen, P. Mogensen, and B. Fleury, "A stochastic model of the temporal and azimuthal dispersion seen at the base station in outdoor propagation environments," *IEEE Trans. Veh. Technol.*, vol. 49, pp. 437–447, Mar. 2000.
[20] R. Clarke, "A statistical theory of mobile-radio reception," *Bell Syst. Tech. J.*, vol. 47, pp. 957–1000, July 1968.
[21] K. Pedersen, E. Preben, and B. Fleury, "Spatial channel characteristics in outdoor environments and their impact on BS antenna system performance," in *Proc. IEEE Vehicular Technology Conf.*, Edmonton, AB, Canada, May 1998, pp. 719–723.
[22] W.-Y. Lee, "Effects on correlation between two radio base-station antennas," *IEEE Trans. Commun.*, vol. COM-21, pp. 1214–1224, Nov. 1973.
[23] K.-W. Yip and T.-S. Ng, "Karhunen–Loève expansion of the WSSUS channel output and its application to efficient simulation," *IEEE J. Select. Areas Commun.*, vol. 15, pp. 640–646, May 1997.